After the 1000h test, the remaining eight diodes showed no facet damage. Again, the failed lasers could have been selected with a 200h burn-in, using $(I/I_0) > 150\%$ or degradation rates $\beta > 2 \times 10^{-3}$/h as a criterion.

In summary, extension of the vertical near field and facet protection with $ZnSe/Al_2O_3$ enhanced the facet stability. Long resonators allowed stable monomode emission above 300mW. Aging tests at 40 and 70°C demonstrate that in this way, with output powers ≥ 250mW, high long-term stability could be achieved for 'conventional' InGaAs/GaAs/AlGaAs–RW lasers. The low internal optical losses and temperature sensitivity allowed manufacturing of laser diode chips with 3.35mm cavity length. To the best of our knowledge, the stable emission level presented of 'pure' AlGaAs lasers is the best achieved to date for RW lasers.

Acknowledgments: This study has been supported by the German Ministry of Education, Sciences, Research and Technology (BMBF) under contract no. 01 BP 447. The authors would like to thank T. Tessaro, I. Fechner, N. Herrfurth, A. Krause, R. Olschewski, R. Selent and P. Wochatz for their assistance in growing, processing, mounting and measuring the laser diodes.

13 March 1998
Electronics Letters Online No: 19980581

G. Beister, F. Bugge, G. Erbert, J. Maege, P. Ressel, J. Sebastian, A. Thies and H. Wenzel (*Ferdinand-Braun-Institut für Höchstfrequenztechnik, Rudower Chaussee 5, D-12489 Berlin, Germany*)

References

1 OOSENBRUG, A., HARDER, C.S., JAKUBOWICZ, A., and ROENTGEN, P.: 'Power integrity of 980nm pump lasers at 200mW and above'. Proc. 9th Annual Meeting IEEE Lasers and Electro-Optics Society, LEOS '96, Boston, MA, USA, 18–21 November 1996, Paper TuZ3, pp. 348–349

2 BURKHARDT, H., PIATAEV, V., and SCHLAPP, W.: 'High power, high T_0 oxide stripe-geometry 980-nm laser diodes'. SPIE Proc. Series, Laser Diodes and Application II, 1996, Vol. 2682, pp. 11–19

3 SAVOLAINEN, P., TOIVONEN, M., ASONEN, H., PESSA, M., and MURISON, R.: 'High-performance 980-nm strained-layer GaInAs-GaInAsP-GaInP quantum-well lasers grown by all solid-source molecular-beam epitaxy', *IEEE Photonics Technol. Lett.*, 1996, **8**, (8), pp. 986–988

4 DUTTA, N.K., HOBSON, W.S., VAKHSHOORI, D., HAN, H., FREEMAN, P.N., DE JONG, J.F., and LOPATA, J.: 'Strain compensated InGaAs-GaAsP-InGaP laser', *IEEE Photonics Technol. Lett.*, 1996, **8**, (7), pp. 852–854

5 ERBERT, G., BEISTER, G., BUGGE, F., MAEGE, J., RESSEL, P., SEBASTIAN, J., VOGEL, K., WENZEL, H., and WEYERS, M.: 'Stable operation of InGaAs/InGaP/AlGaAs (λ = 1020nm) laser diodes', *Electron. Lett.*, 1997, **33**, pp. 778–779

6 CHAND, N., HOBSON, W.S., DE JONG, J.F., PARAYANTHAL, P., and CHAKRABARTI, U.K.: 'ZnSe for mirror passivation of high power GaAs based lasers', *Electron. Lett.*, 1996, **32**, pp. 1595–1596

Noise in passively mode-locked lasers

D. Eliyahu and A. Yariv

For the first time, phase fluctuations in the spectral intensity of the pulse train generated by passively mode-locked semiconductor lasers have been measured. The results reveal diffusion-like fluctuations of this phase. The timing jitter fluctuations were also measured, and, in contrast, have a correlation time which is much longer than the repetition time.

Noise in mode-locked lasers limits system performance. An understanding of such noise is therefore of importance in applications such as optical data transmission, electro-optic sampling and free space and fibre ranging. The effect of timing-jitter fluctuations on the power spectrum of passive mode locking has previously been studied [1, 2]. It was found that, when timing-jitter fluctuations between successive neighbouring pulses are uncorrelated in time, Lorentzian-shaped spectra at the different harmonics of the pulse repetition frequency, with FWHM proportional to the square of the harmonic number, will result [2]. Correlations between the timing fluctuations of different pulses in the train tend to produce spectra which are both Gaussian in shape and have FWHMs that increase linearly with harmonic number (when the harmonic number is greater than a minimum value that depends on the repetition time, RMS timing jitter fluctuations and correlation time [2]). Amplitude fluctuations were found to have a small effect on the power spectrum, and mainly extend the wings of the spectra.

In this Letter, we show that pulse-to-pulse phase fluctuations of the spectral intensity are important in these lasers and can be revealed by examining the power spectrum. The phase noise results from pulse shape fluctuations. To measure the noise characteristics, we performed a spectral analysis of the detected photocurrent as measured by a photodetector followed by a radio frequency spectrum analyser. The detected power spectrum at angular frequency ω is [2]

$$P_I(\omega) = \lim_{N\to\infty} \frac{1}{2N+1} \sum_{k,l=-N}^{N} \langle F_k(\omega) F_l^*(\omega) \exp[i\omega(T_k - T_l)] \rangle \tag{1}$$

where $F_k(\omega)$ describes the Fourier transform of the intensity envelope of the kth pulse in the train, which occurs at time T_k. In the presence of phase fluctuations of the spectral intensity, and assuming that amplitude fluctuations have a small effect on the power spectrum [2], we can replace $F_k(\omega)$ by $F(\omega)\exp(i\phi_k)$, where $\phi_k(\omega)$ is the spectral intensity phase of the kth pulse, and $F(\omega)$ is the average absolute value of $F_k(\omega)$. Assuming that $\phi_k(\omega)$ has Gaussian diffusion-like fluctuations (no correlations), where

$$\langle [\phi_k(\omega) - \phi_l(\omega)]^2 \rangle = 2\alpha(\omega)|k-l| \tag{2}$$

and the timing jitter has Gaussian fluctuations with long correlation time [2], then the power spectrum is given by

$$\begin{aligned} P_I(\omega) &= |F(\omega)|^2 \lim_{N\to\infty} \frac{1}{2N+1} \sum_{k,l=-N}^{N} \exp[-\alpha(\omega)|k-l|] \\ &\quad \times \exp\left[-\frac{\omega^2}{2}\langle \Delta T^2 \rangle |k-l|^2\right] \exp[i\omega T(k-l)] \\ &= |F(\omega)|^2 \left(\frac{2\pi}{\omega^2 \langle \Delta T^2 \rangle}\right)^{1/2} \\ &\quad \times \sum_{n=-\infty}^{\infty} \mathrm{Re}\left\{ \exp\left[\frac{(\alpha(\omega)T + i\Delta\omega_n T)^2}{2\omega^2\langle \Delta T^2\rangle}\right] \mathrm{erfc}\left(\frac{\alpha(\omega)T + i\Delta\omega_n T}{\sqrt{2\omega^2\langle \Delta T^2\rangle}}\right)\right\} \end{aligned} \tag{3}$$

Here, $\alpha(\omega)$ is related to the diffusion constant of the random walk process, $\Delta\omega_n = \omega - \omega_n$ is the offset (angular) frequency of the nth harmonic power spectrum, T is the average repetition time, $\langle \Delta T^2 \rangle^{1/2}$ is the RMS value for the timing jitter fluctuations of adjacent pulses, $\mathrm{Re}(z)$ represents the real part of the complex expression z and $\mathrm{erfc}(z)$ is the complementary error function [3]. The main contribution to the nth harmonic number of the power spectrum is from the nth term in the summation of eqn. 3.

The theoretical result given in eqn. 3 is now compared with experimental results. The InGaAsP/InP laser which was used is a passively mode-locked quadruple quantum well buried heterostructure, lasing at ~1.54μm wavelength. This semiconductor laser has two sections. The first section, which is 2mm long, is forward biased to provide the gain of the laser. The facet on this side has an anti-reflective coating in order to couple the infrared light to the external cavity, formed by a 70% reflection mirror. By reverse biasing the short segment, which is 230μm long, a waveguide saturable absorber is formed. The facet on the absorber side has a highly reflective coating. The two sections are separated by 50μm, with a DC isolation of 1.5kΩ. The external-mirror-to-laser distance controls the repetition rate, which in our case was 528MHz.

The power spectrum of the laser intensity was recorded with a fast microwave photodiode receiver, a microwave amplifier and an electronic spectrum analyser. The normalised spectra of different harmonics are shown in Fig. 1 as a function of the offset frequency divided by the harmonic number n. The solid curves describe the theoretical fitting to the experiment. Measurements could not be taken for the first harmonic due to RF pick-up and low photodiode and amplifier response below 1GHz.

Eqn. 3 was used to fit the experimental results of the power spectrum measurement. The fitting parameters are $\langle \Delta T^2 \rangle^{1/2}/T = 3.6 \times 10^{-4}$, $\alpha_2 = 0.035$, $\alpha_3 = 0.028$, $\alpha_4 = 0.022$, and $\alpha_{n>4} = 0.03$, where $\alpha_n = \alpha(\omega_n)$. The timing jitter correlation time τ_j is assumed to be long such that $\tau_j/T > 625$, hence all harmonic numbers starting from $n = 1$ are strongly influenced by the parabolic shape of the timing jitter noise, as found previously for a similar system [2].

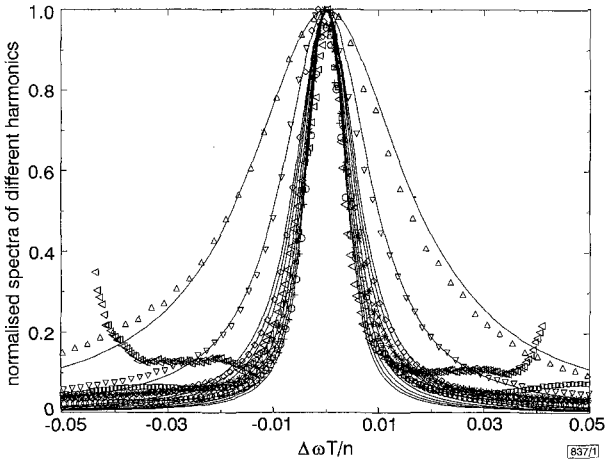

Fig. 1 *Normalised intensity spectra of different harmonics against offset frequency divided by harmonic number n*

Theoretical results of eqn. 3
△ $n = 2$ × $n = 7$
▽ $n = 3$ ✳ $n = 8$
◇ $n = 4$ □ $n = 12$
○ $n = 5$ ◁ $n = 20$
\+ $n = 6$ ——— theory

Defining $\tau_D(\omega)$ as the diffusion time of the phase fluctuations in the spectral intensity at angular frequency ω, it is related to $\alpha(\omega)$ by:

$$\tau_D(\omega) = \frac{T}{\alpha(\omega)} \tag{4}$$

In our case, $1/\tau_D(\omega)$ varies between 11.6 and 18.5MHz, depending on the harmonic number. These values imply that the source for these fluctuations is spontaneous emission and that it varies strongly for different frequencies.

In conclusion, we have shown that timing jitter fluctuations have a correlation time that is much longer than the repetition time. The phase of the spectral intensity has a short correlation time and relatively strong frequency dependence.

Acknowledgment: This research was supported by the Advanced Research Projects Agency.

9 February 1998
Electronics Letters Online No: 19980531

D. Eliyahu and A. Yariv (*California Institute of Technology, M/S 128-95, Pasadena, California, USA*)

D. Eliyahu: currently with Waveband Corporation, 375 Van Ness Avenue, Suite 1105, Torrance, CA 90501, USA

References

1 HAUS, H.A., and MECOZZI, M.: 'Noise of mode-locked lasers', *IEEE J. Quantum Electron.*, 1993, **QE-29**, pp. 983–996
2 ELIYAHU, D., SALVATORE, R.A., and YARIV, A.: 'Effect of noise on the power spectrum of passively mode-locked lasers', *J. Opt. Soc. Am. B, Opt. Phys.*, 1997, **14**, pp. 167–174
3 GRADSHTEYN, I.S., and RYZHIK, I.M.: 'Table of integrals, series and products' (Academic, New York, 1965), 4th edn.

UV trimming of arrayed-waveguide grating wavelength division demultiplexers

D.A. Zauner, J. Hübner, K.J. Malone and M. Kristensen

The transmission peak wavelength of a fibre-pigtailed arrayed-waveguide silica-on-silicon grating (AWG) demultiplexer has been shifted using a 248nm excimer laser without penalties in crosstalk or insertion loss. The transmission peak shift and shape were monitored while trimming. A wavelength shift of 0.77nm (94GHz) was achieved while keeping a crosstalk of –25dB for 400GHz channel spacing and an insertion loss < 7dB.

Introduction: The main characteristics of an integrated optical demultiplexer are insertion loss, transmission peak wavelength, channel spacing and channel crosstalk. Components with excellent crosstalk characteristics may be of little use if the peak wavelength due to process deviations is far from the design value, typically a wavelength on the ITU grid. Thermal tuning is feasible but has its drawbacks. Due to the small order of magnitude of the thermo-optic coefficient of silica it may take several watts of electrical power to adjust a silica-on-silicon device to the ITU grid. After adjustment, the device requires a continuous temperature control to keep it on grid, which makes thermal tuning impractical for some applications. In this Letter, we demonstrate precise control of the peak wavelength of an integrated optical multiplexer after fabrication by UV-inducing permanent changes in the optical path length differences in an arrayed-waveguide grating demultiplexer.

Principle and experiment: An AWG demultiplexer consists of an array of singlemode waveguides connecting two focusing slab waveguides (Fig. 1). The wavelength dispersion is achieved by introducing a constant length difference ΔL between adjacent waveguides in the array and, hence, a wavelength-dependent phase shift [1]. In this way, a wavelength-dependent wavefront tilt is produced in the second slab waveguide. The position of the point to which this new wavefront converges is then different for each wavelength, causing a multiwavelength signal to be demultiplexed to different output ports. Due to process variations the refractive index and waveguide dimension can only be controlled within certain limits. This causes the effective optical path lengths of the array waveguides to differ from the nominal values. The centre wavelength λ_c is defined according to

$$n_c \Delta L = m\lambda_c \tag{1}$$

where n_c is the effective index of the waveguide and m is the diffraction order. We now add a constant optical path length difference ΔL_{uv} by UV inducing refractive index changes through a triangular mask (Fig. 1). In this configuration ΔL_{uv} will decrease the effective optical length difference between the waveguides and the centre wavelength decreases.

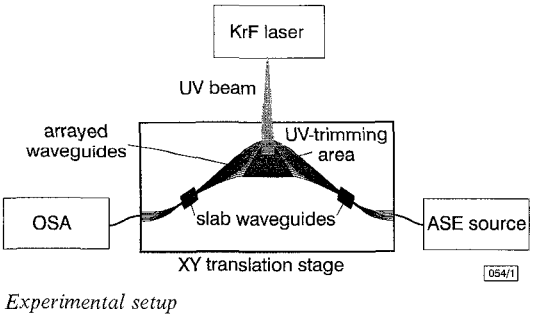

Fig. 1 *Experimental setup*

We used the experimental setup shown in Fig. 1. A 248nm KrF excimer laser was used as UV source and the trimming was performed on a 400GHz channel spacing pigtailed demultiplexer fabricated using plasma enhanced chemical vapour deposition (PECVD) silica-on-silicon. The 6×6μm² GeO_2 cores have a relative